This is a preprint submitted to EarthArxiv. The paper is currently under review.

A Shallow Water Model for Convective Self-Aggregation

Da Yang*

University of California, Davis; Lawrence Berkeley National Laboratory

**Corresponding author address:* 253 Hoagland Hall, University of California, Davis, California, USA.

E-mail: dayang@ucdavis.edu

ABSTRACT

Convective self-aggregation is proposed to be fundamental to the development of tropical cyclones and the Madden-Julian Oscillation, both of which are long-term mysteries in tropical meteorology. Therefore, understanding self-aggregation is key to deciphering how convection works in the tropical atmosphere. Here we present a 1D shallow water model that simulates the dynamics of the planetary boundary layer. We parameterize convection as a small-scale, short-lived mass sink that is triggered when the layer thickness exceeds a certain threshold. Once triggered, convection lasts for finite time and occupies finite length. We show that the model can successfully simulate self-aggregation, and that the results are robust to a wide range of parameter values. By analyzing the available potential energy budget (APE), we show convection generates APE, providing energy for self-aggregation. This paper provides a simple modeling framework to study self-aggregation, which can be used to understand the temporal and spatial scales of self-aggregation.

1. Introduction

Persistent convectively coupled circulations can self-emerge over an ocean surface with uniform temperature (Held et al. 1993; Bretherton et al. 2005). These circulation patterns are sustained by significant buoyancy and pressure gradients in the planetary boundary layer (Yang 2018a,b). Intense thunderstorms are ubiquitous in the upwelling branch of the circulation; clear sky conditions prevail in the downwelling branch of the circulation. This phenomenon is known as convective self-aggregation and has been extensively simulated in computer models (Muller and Held 2012; Wing and Emanuel 2014; Holloway and Woolnough 2016; Yang 2019).

A suite of studies have suggested that physical processes that lead to and maintain self-aggregation are key to the development of tropical cyclones (Wing et al. 2016; Boos et al. 2016) and the Madden-Julian Oscillation (MJO) (Yang and Ingersoll 2013, 2014; Arnold and Randall 2015; Pritchard and Yang 2016; Khairoutdinov and Emanuel 2018), which are long-term mysteries in tropical meteorology. Understanding physics of self-aggregation, therefore, would help us decipher how convection interacts with atmospheric circulations in the tropics.

Recent progress in understanding self-aggregation primarily relies on cloud-resolving models (CRMs) and general circulation models (GCMs) (Bretherton et al. 2005; Muller and Held 2012; Muller and Bony 2015; Yang 2018a, 2019, 2018b; Arnold and Putman 2018; Patrizio and Randall 2019). These studies have suggested that a number of physical processes can affect the development of self-aggregation, including feedbacks involving radiation, surface fluxes, water vapor, convective heating, and evaporation of rain. Studies have also suggested that, at steady state, there is a natural length scale of self-aggregation, which is of O(2000 km) in the current climate (Wing and Cronin 2015; Yang 2018b; Patrizio and Randall 2019; Arnold and Putman 2018).

However, there are no simple models that can capture all basic features of self-aggregation. Some models focused on developing instability mechanisms responsible for the initial growth of aggregated circulations (Bretherton et al. 2005; Craig and Mack 2013; Emanuel et al. 2014; Beucler and Cronin 2016; Yang 2018a; Windmiller and Craig 2019), and other models focused on what maintains the circulation and sets the spatial scale at steady state (Yang 2018b; Wing et al. 2016; Arnold and Putman 2018; Patrizio and Randall 2019). There lacks a simple model that simulates the entire aggregation process, from the onset to the steady state.

Recent studies suggested that PBL diabatic processes are key to the development of self-aggregation (Naumann et al. 2017; Yang 2018a), and that horizontal buoyancy and pressure gradients in the PBL maintain the steady-state circulation (Yang 2018b; Arnold and Putman 2018; Patrizio and Randall 2019). Motivated by these studies, we present a 1D shallow water model that simulates atmospheric flows in the planetary boundary layer (PBL), roughly the lowest 2 km. With a simple convection parameterization, this model can simulate convective self-aggregation to a statistically steady state from a homogeneous initial condition. We propose that the convective heating–overturning circulation (CHOC) feedback provides energy to self-aggregated circulations, which is consistent with recent CRM results (Yang 2018a, 2019).

As a starting point, the current model focuses on reproducing the minimal simulation in Figure 7 of Yang (2018a). In that simulation, convection self-aggregates without radiative, surface-flux, and vapor-buoyancy feedbacks, and evaporation of rain. Building complexity on this shallow water model will be left for future work.

2. A Boundary Layer Framework

We briefly review the PBL framework for self-aggregation (Naumann et al. 2017; Yang 2018a,b; Arnold and Putman 2018; Patrizio and Randall 2019). Yang (2018a) discovered that the development of convective self-aggregation is associated with increase of available potential energy (APE), which is due to the generation of APE. The generation of APE, also known as the APE production, is a process of amplifying buoyancy anomalies: heating (cooling) the warm (cold) part of the atmosphere generates APE (Vallis 2017). The APE production then requires horizontal buoyancy anomalies. In the absence of rotation, there is no force to balance horizontal buoyancy and pressure gradients in the free troposphere, so buoyancy and pressure perturbations can be effectively smoothed out by gravity waves (Charney 1963; Sobel et al. 2001; Yang and Seidel 2020). Therefore, the APE production is primarily in the PBL, which then becomes critical to the development of self-aggregation. This hypothesis was confirmed by using a suite of mechanism-denial CRM simulations (Yang 2018a).

Yang (2018b) developed a theory for what sets the horizontal scale of self-aggregation by considering dominant balances in the PBL. This theory suggests that the size of self-aggregation scales with PBL height and the square root of buoyancy variation in the PBL. This theory correctly predicts that the natural length scale of self-aggregation is of O(2000 km), and explains how the spatial scale of self-aggregation varies with climate change (see his Figs. 3 & 10). Although this theory was developed in a 2D atmosphere, it has been subsequently used to explain 3D simulation results (Arnold and Putman 2018; Patrizio and Randall 2019).

This PBL framework is supported by a growing body of literature showing the importance of PBL in leading to self-aggregation (Bretherton et al. 2005; Muller and Bony 2015; Naumann et al. 2017; Colin et al. 2019) and in maintaining the steady-state circulations (Arnold and Putman 2018; Patrizio and Randall 2019). These recent studies justify the idea of constructing a shallow water model to simulate PBL dynamics and thereby self-aggregation.

3. A Shallow Water Model

We construct a linear shallow water model that simulates the dynamics of the PBL. This model only includes a minimum set of ingredients in order to reproduce the basic features of the minimal simulations presented in Yang (2018a), in which radiative, surface-flux, vapor-buoyancy feedbacks, and evaporation of rain are all absent.

In the shallow water model, we represent the effect of convection, radiation, and surface fluxes in the continuity equation, which acts as the thermodynamic equation (Lindzen and Nigam 1987; Gill 1980). We then represent convection as a small-scale mass sink and represent the overall effect of radiation and surface fluxes as a constant and uniform mass source to the shallow water model (no radiative and surface-flux feedbacks). In a statistically steady state, the mass sink should balance the mass source averaged over the entire domain, which can be considered as the radiative-convective equilibrium (RCE) in this shallow water model.

There are different ways to interpret why we can represent convection as a mass sink for our shallow water model. First, when convection occurs, there are small-scale upward mass fluxes from the PBL to the free troposphere, which is a mass sink of the PBL indeed. Second, we can view that our shallow water model simulates the lower branch of an overturning circulation roughly with a first-baroclinic vertical structure. Then convective heating is mathematically equivalent to a mass sink to the PBL (our model) or a mass source to the upper troposphere (Gill 1980; Lindzen and Nigam 1987; Kuang 2008; Yang and Ingersoll 2013): convective heating lowers surface pressure. The overall effect of radiation and surface-fluxes does the opposite to convection, so we repsent it as a mass source.

The governing equations of our shallow water model are given by

$$\partial_t u = -\phi_x - u/\tau_d, \tag{1}$$

$$\partial_t \phi + c^2 \partial_x u = F_c + F_l - (\phi - \bar{\phi})/\tau_d, \tag{2}$$

where u represents horizontal velocity (m/s^2); ϕ represents geopotential (m^2/s^2), and $\bar{\phi}$ represents its domain average; τ_d represents a linear damping timescale (1/s); c represents the gravity wave speed (m/s); F_c represents convective heating (m^2/s^3), which is parameterized as a mass sink, F_l represents large-scale forcings that are constant in time and space (m^2/s^3), parameterized as a mass source.

Before we provide details of the convection parameterization, we discuss a few important assumptions and simplifications. First, we assume that linear dynamics is sufficient to capture convective self-aggregation, because nonlinear contributions to the development of self-aggregation seem to be negligible in CRM simulations [see the APE analysis in Yang (2018a, 2019)]. Second, we assume linear damping in both u and ϕ. Although highly idealized, the linear damping seems to capture the overall damping effect at a wide range of lengthscales [see Fig. 10 of Kuang (2012)]. Similar to previous studies, here we use the same damping timescale for both u and ϕ for simplicity (Gill 1980; Neelin 1989). Third, we parameterize the overall effect of radiative cooling and surface fluxes as a uniform mass source F_l, mimicking the minimal simulation in Yang (2018a), in which there are no radiative and surface-flux feedbacks. Last, we assume that a prognostic moisture equation is not necessary. This is because the moisture-entrainment-convection feedback seems to be secondary for self-aggregation (Arnold and Putman 2018; Yang 2019).

We parameterize convection as a triggered process (Fig. 1) following Yang and Ingersoll (2013, 2014), who have sucessfully simulated spontaneous development of the MJO. When ϕ exceeds a threshold ϕ_c, convection is triggered, and latent heat is released. Each convective event occupies a finite length ($2r_c$) and lasts for a finite time (τ_c):

$$F_c = -\frac{q}{r_c \times \tau_c} \times \left[1 - \left(\frac{\Delta t - \tau_c/2}{\tau_c/2}\right)^2\right] \times \left(1 - \frac{r^2}{r_c^2}\right), \tag{3}$$

where q measures the amplitude of convection (a positive number), Δt represents the time interval since the onset of convection, and r represents the distance of a location to the convective center. F_c is zero when $\Delta t > \tau_c$ or $r > r_c$ (Fig. 1).

This convection parameterization is almost identical to that in Yang and Ingersoll (2013, 2014), who have successfully simulated the MJO in a shallow water model. The only difference is that we parameterize the effect of convection on the PBL (the lowest 2 km), whereas Yang and Ingersoll (2013, 2014) focused on the upper troposphere. This convection scheme has been referred to as triggered convection, in contrast to quasi-equilibrium (QE) convection (Emanuel et al. 1994). Convective heating is not an instantaneous function of the thermodynamic state nor the PBL convergence. This convection scheme is, therefore, also different from the conditional instability of the second kind (CISK) (Bretherton 2003; Emanuel et al. 1994). This convection scheme proposes that convection would occur only if enough mass has been accumulated in the PBL ($\phi > \phi_c$). This implies that convection lags the PBL convergence. This lag could be due to the sensitivity of deep convection to moisture and convective available potential energy (CAPE), both of which favor deep convection. Therefore, ϕ in our model has implicitly included information of moisture.

Here convection is triggered by *small-scale* high pressure anomalies. At first sight, this seems to be surprising because convection often occurs at low pressure areas. However, we will show that convection indeed occurs in *large-scale* low pressure environment in our shallow water simulations (Section 4). Although convection is triggered when ϕ is higher than ϕ_c, ϕ quickly falls below ϕ_c and then keeps falling until $\Delta t = \tau_c$. Therefore, convection lowers the layer thickness in an area with anomalously low ϕ during most of the convecting period. This is key to generate the large-scale low-pressure environment and to simulate convective self-aggregation. We will further illustrate how convection works by using our simulation results (Section 4).

In this shallow water model, fluid dynamics is linear, and the only nonlinearity comes from the triggered convection. Therefore, the absolute amplitude of any forcing is not of interest. This is because we can scale the entire equation by any arbitrary factor, and the dynamics should remain identical. There are five free parameters: convective timescale τ_c, radius of convective storms r_c, gravity wave speed c, and the damping timescale τ_d, number density of convective events S_c. S_c is a derived parameter, measuring number of convective events per unit area per time. Over a time period T and a spatial scale L, the energy balance is given by

$$n \times q \sim F_l \times T \times L, \tag{4}$$

where n represents number of convective events over T and L. S_c then emerges from this energy balance:

$$S_c \equiv \frac{n}{T \times L} \sim \frac{F_l}{q}. \tag{5}$$

Here we have used that the integrated effect of individual storms over its entire life cycle and convective area scales with q, which has been carefully discussed in Yang and Ingersoll (2013, 2014). We have dropped an $O(1)$ scaling factor in the above analysis, which makes the physics more transparent and does not affect the rest of the paper.

We choose a set of reference parameter values: $\tau_c = 0.6$ hr, r_c = 10 km (the size of a storm is $2 \times r_c = 20$ km), $S_c = 4 \times 10^{-10}$ m^{-1} s^{-1} (about 276 storms per day over the entire domain), $c = 20$ m/s, and $\tau_d = 1$ day. The parameter values are similar to those in Yang and Ingersoll (2013, 2014). In order to test the robustness of simulation results, we have varied all parameter values at least by a factor of 2.

We integrate the shallow water model using the Lax-Wendroff method with the grid spacing $\delta x = 5$ km and time step $\delta t = 1$ min. For the reference parameter values, there are 5 grid points and 36 time steps within a convective storm, which is then well resolved. We have tested the sensitivity to δx and δt, and the simulation results remain almost unchanged by using higher resolutions.

4. Simulation Results

Our shallow water model can successfully simulate spontaneous organization of large-scale circulations and convection. Figure 2 shows ϕ, convection, and u of the reference simulation. Large-scale structures in convection and circulation self-emerge quickly, reaching a statistically steady state around day 30. Convective centers collocate with large-scale low pressure centers and convergence, which is consistent with results in CRM simulations [see Fig. 2 in Yang (2018a)]. Within the large-scale envelopes, there are small-scale, short-lived gravity waves excited by convective storms. These gravity waves propagate toward opposite directions at the same speed, forming standing wave patterns that meanders slowly.

To further illustrate how our convection scheme works, we plot a snapshot of ϕ and F_c in Fig. 3a. Convection is triggered when ϕ exceeds ϕ_c locally. This is evident, for example, at $x \approx 2500$ km and at $x \approx 4500$ km (the small orange dips). These storms span $2r_c = 20$ km in x (a much smaller scale than the convective aggregates) and will last for $\tau_c = 0.6$ hours once triggered. The amplitude of convective heating evolves with time according to (3), which is also illustrated in Fig. 1b. It will first increase and then decrease back to 0 when $\Delta t = \tau_c$. The big orange dips (*e.g.*, at $x \approx 4500$ km and $x \approx 7000$ km) represent convective heating around the mature stage ($\Delta t = \tau_c/2$). ϕ at these locations already becomes much lower than ϕ_c due to the effect of convection. Although triggered by high ϕ, convection lowers the layer thickness in an area with anomalously low ϕ during most of the convecting period.

The convective storms excite small-scale gravity waves, which then form large-scale wave envelopes (Figs. 2a, 2c and 3a). To better illustrate this multi-scale structure, we decompose ϕ according to

$$\phi(t,x) = \overline{\phi}(t) + \phi'(t,x),\ \phi' = \widetilde{\phi} + (\phi' - \widetilde{\phi}), \tag{6}$$

where $\overline{\phi}(t)$ represents domain-averaged ϕ, which is very close to c^2; ϕ' represents perturbations around $\overline{\phi}$; $\widetilde{\phi}$ represents slowly varying components of geopotential anomalies (Fig. 3b, calculated as a 5-day average); and $(\phi' - \widetilde{\phi})$ represents fast components of geopotential anomalies (Fig. 3c), which are mostly gravity waves. The slow components have clear large-scale structures, corresponding to convective aggregates (Fig. 3b). The fast components have two length scales. The fine-scale structures are associated with individual gravity waves, and the large-scale features are wave packets–a group of gravity waves that travel together (Fig. 3c). Because these gravity waves propagate to opposite directions with the same speed, the wave packets are almost stationary in space.

These gravity waves are excited by convection, and their energy–the amplitude of waves–concentrates around convective centers (Fig. 3c), which helps trigger new convective storms nearby. This is essentially the aggregation mechanism proposed in Yang and Ingersoll (2013). The collective effect of individual storms rectifies to a large-scale mass sink, producing a large-scale low pressure environment (Fig. 3b): statistically, convection resides in a large-scale low pressure environment indeed.

We apply running average in time and space with the window widths as 5 days and 100 km, respectively. This filters out gravity waves and highlights the large-scale circulations (Figs. 2d-f). It becomes clearer that the envelope of convective heating coincides with low pressure centers throughout the entire simulation. This suggests that, at the large scale, convection generates APE, providing energy for self-aggregation.

Before we perform detailed APE analysis, we test the parameter sensitivity of our results. In each simulation, we only vary one parameter and keep the other parameters identical to those in the reference simulation. In Fig. 4, the first column presents simulations with $\tau_c = 0.4$, 0.6, and 1 hour, respectively. The second column presents simulations with $r_c = 10$, 20, and 40 km, respectively. The third column presents simulations with $\tau_d = 0.5$, 1, and 2 days, respectively. The fourth column presents simulations with $S_c = 2\times10^{-10}$, 4×10^{-10}, 8×10^{-10} m^{-1} s^{-1}. The fifth column presents simulations with $c = 15,\ 20,\ 30$ m/s. We have varied each parameter at least by a factor of 2.

Figure 4 shows horizontal wind u in a suite of simulations with a wide range of parameter values. All simulations have reproduced basic features of convective self-aggregation simulated by CRMs. Convection can self-aggregate from an initially homogeneous state, and the large-scale circulation pattern persists and reaches a (quasi-) steady state. The spatial scale of convective aggregates is about 2000 km - 4000 km, consistent with 2D CRM results Yang (2018b).

In all simulations, there are small-scale, short-lived gravity waves within the large-scale circulation pattern. The gravity waves propagate to both directions at $c = 15-30$ m/s, whereas the large-scale pattern remains almost in place or meanders slowly without a preferred direction. For example, in Fig. 4a, the gravity wave speed is 20 m/s (the black line). The large-scale circulation drifts to the right at about 3 m/s during the first 30 days of the simulation and then drifts to the left with the same speed for another 30 days. Such slow propagation was also observed in CRM simulations (e.g., Fig. 7 in Yang (2018a)). Given that the maximum propagation speed is only about 15% of c, and that there is no preferred direction, this slow propagation is not of our interest.

In Fig. 4b, there are abrupt shifts in locations of large-scale convergence (precipitation) centers (e.g., around day 20, 40, and 80). In CRM simulations, such abrupt shifts rarely occur unless there are significant horizontal winds (e.g., Fig. B3 in Yang (2018a)). This is because moisture helps localize convection: humid environment favors convection, and its associated large-scale circulations then further moisten the environment (Tompkins 2001). Here, the drift rate compares to c, so these abrupt shifts are likely related to gravity waves.

The spatial scale varies when we change parameter values in Fig. 4. For example, when increasing τ_d or c, convective aggregates become larger (the third and fifth columns in Fig. 4). This seems to suggest that the spatial scale $l \sim c \times \tau_d$. Using $c = 20$ m/s and $\tau_d = 1$ day, we get $l = 1728$ km, which is consistent with the characteristic length scale of the simulated convective aggregates. However, the spatial scale also changes when we vary other parameters. For example, l decreases with increasing S_c (the fourth column in Fig. 4), suggesting $l \sim \sqrt{c/S_c}$, which was proposed by Yang and Ingersoll (2014). To test which scale sets the spatial scale of convective aggregates, we need a suite of large-domain simulations that can accommodate 10+ convective aggregates, so that the domain size is much larger than l and no longer affects the scaling results. Therefore, we leave this investigation to a future study.

In summary, we have successful simulated convection self-aggregation in a shallow water model with a wide range of parameter values. The gross features of the simulated aggregates resemble those in CRM simulations, although details may differ (e.g., the abrupt shift of precipitation centers).

5. Available Potential Energy Analysis

Now we focus on the reference simulation and try to understand what provides energy for the development and maintenance of self-aggregation at the large scale. We analyze the APE (J/kg) budget, following Yang (2018a, 2019). In the shallow water system, we define

$$\mathrm{APE} = \frac{\overline{\phi'^2}}{2c^2}, \tag{7}$$

where $\phi' \equiv \phi - \bar{\phi}$, and $\overline{\phi}$ represents the domain average of ϕ (Gill 1982). This APE formulation corresponds well with that of a continuously stratified atmosphere [e.g., (1) in Yang (2018a)]: ϕ' is related to the buoyancy perturbation, and c^2 measures stratification.

We can derive the APE budget for convective self-aggregation, which is given by

$$\overbrace{\partial_t \frac{\overline{\widetilde{\phi'}^2}}{2c^2}}^{\partial_t \mathrm{APE}} + \underbrace{\overline{\widetilde{\phi'}\partial_x \tilde{u}}}_{\text{Conversion to KE}} = \overbrace{\frac{\overline{\widetilde{F_c'}\widetilde{\phi'}}}{c^2}}^{\text{APE Production}} - \underbrace{\frac{\overline{\widetilde{\phi'}^2}}{c^2 \tau_d}}_{\text{APE Sink}}, \tag{8}$$

where $\widetilde{(\cdot)}$ represents a slowly varying component associated with self-aggregation Yang (2018a); $F_c' = F_c - \bar{F}_c$.

Figure 5a shows the evolution of APE. The evolution of APE generally synchronizes with the development of convective self-aggregation. In the beginning of the simulation, APE is negligible because of the uniform initial condition. However, APE rapidly increases with time around day 7, when large-scale organization starts to appear. APE reaches a local minimum around day 20, when the aggregated circulation weakens; APE starts to grow again when the aggregated circulation strengthens. The APE oscillates around a reference value after day 40, when the aggregated circulation reaches a statistically steady state. This is in good agreement with Yang (2018a, 2019), suggesting the process of self-aggregation is associated with APE evolution.

We further show that convective heating coincides with ϕ', generating APE and providing energy for self-aggregation. Figure 5b plots

$$\sigma = \frac{(8)}{\mathrm{APE}}, \tag{9}$$

where σ is an inverse timescale, characterizing the efficiency of generating APE due to individual processes. Larger σ indicates a shorter timescale (higher efficiency). We find that convective heating is most efficient in generating APE. Once APE is generated, a large fraction of it is quickly converted to KE, forming circulations. The sink of APE is due to the linear damping in (3): $\sigma_{\text{sink}} = 2/\tau_d = 4\ \text{day}^{-1}$. The sum of all above contributions leads to slow changes in APE with time.

Figure 5 agrees well with Figs. 3-4 in Yang (2018a) and Fig. 3 in Yang (2019), which show APE evolution in CRM simulations. This agreement supports that the CHOC feedback provides energy for the development of self-aggregation.

6. Conclusion and discussion

This paper presents a shallow water model to simulate the PBL circulation of convective self-aggregation. The simulation results resemble those of CRM simulations, and we show that the simulation results are robust to a wide range of parameter values. A key component of this model is the triggered convection, which are intermittent and energetic. The convective storms interact with gravity waves, leading to new storms in the vicinity of old storms. This is a process of generating available potential energy and forming convective self-aggregation. Our results agree with Yang (2018a, 2019): the CHOC feedback provides energy for the development and maintenance of convective self-aggregation.

Our model is consistent with the broadly-defined conditional instability of the second kind (CISK), a cooperative instability between atmospheric flows and convection that does not require radiative and surface-flux feedbacks (Bretherton 2003; Mapes 2000; Wu 2003; Kuang 2008). However, there are important differences. First, simple CISK models often parameterize convection in proportion to PBL convergence (of moisture) (Emanuel et al. 1994). In our model, however, convection only occurs once enough mass is accumulated in the lower troposphere, which lags the

PBL convergence. This triggering mechanism could be related to the sensitivity of convection to moisture and/or convective available potential energy (CAPE). Deep convection often occurs when there is enough moisture and CAPE in the atmosphere. Second, CISK models often produces the instability at the grid scale. However, our model produces circulation patterns of thousands of kilometers, similar to those simulated in CRMs. Therefore, the instability in our model due to the CHOC feedback might be distinct from the conventional CISK (Bretherton 2003; Charney and Eliassen 1964; Lindzen 1974).

Our shallow water model can be considered as a non-rotating version of the Yang-Ingersoll model, which reproduces basic features of the MJO (Yang and Ingersoll 2013, 2014). This is consistent with results from convection permitting models: the MJO is a form of self-aggregation over an equatorial β plane (Arnold and Randall 2015; Khairoutdinov and Emanuel 2018). This agreement suggests that the triggered convection scheme might have captured key aspects of how convection interacts with atmospheric flows.

This paper presents a simple modeling framework to study convective self-aggregation, which opens new avenues of research. For example, with only a few free parameters, this model is particularly useful to develop scaling theories for self-aggregation. Following Yang and Ingersoll (2014), we would like to systematically vary all parameters and use the Buckingham Π Theorem to understand what controls the temporal and spatial scales of self-aggregation.

For simplicity, the current model focuses on reproducing the minimal simulation in Yang (2018a) and has, therefore, omitted some physical processes that are known to be important for self-aggregation. In future studies, we would like to construct a more complete model by adding interactive radiation and surface fluxes, and an explicit moisture variable to the shallow water model. The model will then help us gain theoretical insights on the role of radiative and surface-flux feedbacks. It would also be interesting to compare the model results with other theoretical models that focus on radiative feedbacks (Bretherton et al. 2005; Emanuel et al. 2014; Beucler and Cronin 2016).

Acknowledgments. This work was supported by Laboratory Directed Research and Development (LDRD) funding from Berkeley Lab, provided by the Director, Office of Science, of the U.S. Department of Energy under contract DE-AC02-05CH11231. The author was also supported by a Packard Fellowship for Science and Engineering.

References

Arnold, N. P., and W. M. Putman, 2018: Nonrotating convective self-aggregation in a limited area agcm. *Journal of Advances in Modeling Earth Systems*, **10 (4)**, 1029–1046, doi:10.1002/2017MS001218, URL https://agupubs.onlinelibrary.wiley.com/doi/abs/10.1002/2017MS001218, https://agupubs.onlinelibrary.wiley.com/doi/pdf/10.1002/2017MS001218.

Arnold, N. P., and D. A. Randall, 2015: Global-scale convective aggregation: Implications for the Madden-Julian Oscillation. *Journal of Advances in Modeling Earth Systems*, **7 (4)**, 1499–1518, doi:10.1002/2015MS000498, URL http://doi.wiley.com/10.1002/2015MS000498.

Beucler, T., and T. W. Cronin, 2016: Moisture-radiative cooling instability. *Journal of Advances in Modeling Earth Systems*, **8 (4)**, 1620–1640, doi:10.1002/2016MS000763, URL https://agupubs.onlinelibrary.wiley.com/doi/abs/10.1002/2016MS000763.

Boos, W. R., A. Fedorov, and L. Muir, 2016: Convective Self-Aggregation and Tropical Cyclogenesis under the Hypohydrostatic Rescaling. *Journal of Atmospheric Sciences*, **73 (2)**, 525–544, doi:10.1175/JAS-D-15-0049.1, URL http://journals.ametsoc.org/doi/10.1175/JAS-D-15-0049.1.

Bretherton, C. S., 2003: *Wave-CISK*, 1019–1021. Special Publications of the International Union of Geodesy and Geophysics, Elsevier.

Bretherton, C. S., P. N. Blossey, and M. Khairoutdinov, 2005: An Energy-Balance Analysis of Deep Convective Self-Aggregation above Uniform SST. *Journal of the Atmospheric Sciences*, **62 (12)**, 4273–4292, doi:10.1175/JAS3614.1.

Charney, J. G., 1963: A Note on Large-Scale Motions in the Tropics. *Journal of the Atmospheric Sciences*, **20 (6)**, 607–609, doi:10.1175/1520-0469(1963)020⟨0607:ANOLSM⟩2.0.CO;2, URL http://journals.ametsoc.org/doi/abs/10.1175/1520-0469{\%}281963{\%}29020{\%}3C0607{\%}3AANOLSM{\%}3E2.0.CO{\%}3B2.

Charney, J. G., and A. Eliassen, 1964: On the growth of the hurricane depression. *Journal of the Atmospheric Sciences*, **21 (1)**, 68–75, doi:10.1175/1520-0469(1964)021⟨0068:OTGOTH⟩2.0.CO;2.

Colin, M., S. Sherwood, O. Geoffroy, S. Bony, and D. Fuchs, 2019: Identifying the sources of convective memory in cloud-resolving simulations. *Journal of the Atmospheric Sciences*, **76 (3)**, 947–962, doi:10.1175/JAS-D-18-0036.1, URL https://doi.org/10.1175/JAS-D-18-0036.1.

Craig, G. C., and J. M. Mack, 2013: A coarsening model for self-organization of tropical convection. *Journal of Geophysical Research: Atmospheres*, **118 (16)**, 8761–8769, doi:10.1002/jgrd.50674.

Emanuel, K., A. A. Wing, and E. M. Vincent, 2014: Radiative-convective instability. *Journal of Advances in Modeling Earth Systems*, **6 (1)**, 75–90, doi:10.1002/2013MS000270, URL http://doi.wiley.com/10.1002/2013MS000270.

Emanuel, K. A., J. David Neelin, and C. S. Bretherton, 1994: On large-scale circulations in convecting atmospheres. *Quarterly Journal of the Royal Meteorological Society*, **120 (519)**, 1111–1143, doi:10.1002/qj.49712051902, URL http://doi.wiley.com/10.1002/qj.49712051902.

Gill, A. E., 1980: Some Simple Solutions for Heat-Induced Tropical Circulation. *Quart. J. R. Met. Soc.*, **106**, 447–462.

Gill, A. E., 1982: *Atmosphere-Ocean Dynamics*.

Held, I. M., R. S. Hemler, V. Ramaswamy, I. M. Held, R. S. Hemler, and V. Ramaswamy, 1993: Radiative-Convective Equilibrium with Explicit Two-Dimensional Moist Convection. *Journal of the Atmospheric Sciences*, **50 (23)**, 3909–3927, doi:10.1175/1520-0469(1993)050⟨3909:RCEWET⟩2.0.CO;2, URL http://journals.ametsoc.org/doi/abs/10.1175/1520-0469{\%}281993{\%}29050{\%}3C3909{\%}3ARCEWET{\%}3E2.0.CO{\%}3B2http://journals.ametsoc.org/doi/abs/10.1175/1520-0469(1993)050{\%}3C3909:RCEWET{\%}3E2.0.CO;2.

Holloway, C. E., and S. J. Woolnough, 2016: The sensitivity of convective aggregation to diabatic processes in idealized radiative-convective equilibrium simulations. *Journal of Advances in Modeling Earth Systems*, **8 (1)**, 166–195, doi:10.1002/2015MS000511, URL http://doi.wiley.com/10.1002/2015MS000511.

Khairoutdinov, M. F., and K. Emanuel, 2018: Intraseasonal variability in a cloud-permitting near-global equatorial aquaplanet model. *Journal of the Atmospheric Sciences*, **75 (12)**, 4337–4355, doi:10.1175/JAS-D-18-0152.1, URL https://doi.org/10.1175/JAS-D-18-0152.1.

Kuang, Z., 2008: A Moisture-Stratiform Instability for Convectively Coupled Waves. *Journal of the Atmospheric Sciences*, **65 (3)**, 834–854, doi:10.1175/2007JAS2444.1.

Kuang, Z., 2012: Weakly Forced Mock Walker Cells. *Journal of the Atmospheric Sciences*, **69**, 2759–2786, doi:10.1175/JAS-D-11-0307.1.

Lindzen, R. S., 1974: Wave-cisk in the tropics. *Journal of the Atmospheric Sciences*, **31 (1)**, 156–179, doi:10.1175/1520-0469(1974)031⟨0156:WCITT⟩2.0.CO;2.

Lindzen, R. S., and S. Nigam, 1987: On the Role of Sea Surface Temperature Gradients in Forcing Low-Level Winds and Convergence in the Tropics. *Journal of the Atmospheric Sciences*, **44 (17)**, 2418–2436, doi:10.1175/1520-0469(1987)044⟨2418:OTROSS⟩2.0.CO;2, URL http://journals.ametsoc.org/doi/abs/10.1175/1520-0469{\%}281987{\%}29044{\%}3C2418{\%}3AOTROSS{\%}3E2.0.CO{\%}3B2.

Mapes, B. E., 2000: Convective inhibition, subgrid-scale triggering energy, and stratiform instability in a toy tropical wave model. *Journal of the Atmospheric Sciences*, **57 (10)**, 1515–1535, doi:10.1175/1520-0469(2000)057⟨1515:CISSTE⟩2.0.CO;2.

Muller, C., and S. Bony, 2015: What favors convective aggregation and why? *Geophysical Research Letters*, **42 (13)**, 5626–5634, doi:10.1002/2015GL064260.

Muller, C. J., and I. M. Held, 2012: Detailed Investigation of the Self-Aggregation of Convection in Cloud-Resolving Simulations. *Journal of the Atmospheric Sciences*, **69 (8)**, 2551–2565, doi:10.1175/JAS-D-11-0257.1.

Naumann, A. K., B. Stevens, C. Hohenegger, and J. P. Mellado, 2017: A conceptual model of a shallow circulation induced by prescribed low-level radiative cooling. *Journal of the Atmospheric Sciences*, **74 (10)**, JAS–D–17–0030.1, doi:10.1175/JAS-D-17-0030.1, URL http://journals.ametsoc.org/doi/10.1175/JAS-D-17-0030.1.

Neelin, J. D., 1989: On the Intepretation of the Gill Model. URL http://journals.ametsoc.org/doi/abs/10.1175/1520-0469{\%}281989{\%}29046{\%}3C2466{\%}3AOTIOTG{\%}3E2.0.CO{\%}3B2, 2466–2468 pp., doi:10.1175/1520-0469(1989)046⟨2466:OTIOTG⟩2.0.CO;2.

Patrizio, C. R., and D. A. Randall, 2019: Sensitivity of convective self-aggregation to domain size. *Journal of Advances in Modeling Earth Systems*, **0 (ja)**, doi:10.1029/2019MS001672.

Pritchard, M. S., and D. Yang, 2016: Response of the superparameterized Madden-Julian Oscillation to extreme climate and basic state variation challenges a moisture mode view. *Journal of Climate*, JCLI–D–15–0790.1, doi:10.1175/JCLI-D-15-0790.1, URL http://journals.ametsoc.org/doi/abs/10.1175/JCLI-D-15-0790.1.

Sobel, A. H., J. Nilsson, and L. M. Polvani, 2001: The Weak Temperature Gradient Approximation and Balanced Tropical Moisture Waves*. *Journal of the Atmospheric Sciences*, **58 (23)**, 3650–3665, doi:10.1175/1520-0469(2001)058⟨3650:TWTGAA⟩2.0.CO;2.

Tompkins, A. M., 2001: Organization of Tropical Convection in Low Vertical Wind Shears: The Role of Water Vapor. *Journal of the Atmospheric Sciences*, **58 (6)**, 529–545, doi:10.1175/1520-0469(2001)058⟨0529:OOTCIL⟩2.0.CO;2, URL http://journals.ametsoc.org/doi/abs/10.1175/1520-0469(2001)058{\%}3C0529:OOTCIL{\%}3E2.0.CO;2.

Vallis, G. K., 2017: *Atmospheric and Oceanic Fluid Dynamics: Fundamentals and Large-Scale Circulation*. 2nd ed., Cambridge University Press, doi:10.1017/9781107588417.

Windmiller, J. M., and G. C. Craig, 2019: Universality in the spatial evolution of self-aggregation of tropical convection. *Journal of the Atmospheric Sciences*, **76 (6)**, 1677–1696, doi:10.1175/JAS-D-18-0129.1, URL https://doi.org/10.1175/JAS-D-18-0129.1.

Wing, A. A., S. J. Camargo, and A. H. Sobel, 2016: Role of radiative-convective feedbacks in spontaneous tropical cyclogenesis in idealized numerical simulations. *Journal of the Atmospheric Sciences*, JAS–D–15–0380.1, doi:10.1175/JAS-D-15-0380.1, URL http://journals.ametsoc.org/doi/abs/10.1175/JAS-D-15-0380.1.

Wing, A. A., and T. W. Cronin, 2015: Self-aggregation of convection in long channel geometry. *Quarterly Journal of the Royal Meteorological Society*, **142 (694)**, n/a–n/a, doi:10.1002/qj.2628, URL http://doi.wiley.com/10.1002/qj.2628.

Wing, A. A., and K. A. Emanuel, 2014: Physical mechanisms controlling self-aggregation of convection in idealized numerical modeling simulations. *Journal of Advances in Modeling Earth Systems*, **5 (November)**, n/a–n/a, doi:10.1002/2013MS000269, URL http://doi.wiley.com/10.1002/2013MS000269http://dx.doi.org/10.1002/2013MS000269.

Wu, Z., 2003: A Shallow CISK, Deep Equilibrium Mechanism for the Interaction between Large-Scale Convection and Large-Scale Circulations in the Tropics. *Journal of the Atmospheric Sciences*, **60**, 377–392, doi:10.1175/1520-0469(2003)060⟨0377:ASCDEM⟩2.0.CO;2.

Yang, D., 2018a: Boundary layer diabatic processes, the virtual effect, and convective self-aggregation. *Journal of Advances in Modeling Earth Systems*, **10 (9)**, 2163–2176, doi:10.1029/2017MS001261, URL https://agupubs.onlinelibrary.wiley.com/doi/abs/10.1029/2017MS001261, https://agupubs.onlinelibrary.wiley.com/doi/pdf/10.1029/2017MS001261.

Yang, D., 2018b: Boundary layer height and buoyancy determine the horizontal scale of convective self-aggregation. *Journal of the Atmospheric Sciences*, **75 (2)**, 469–478, doi:10.1175/JAS-D-17-0150.1, URL https://doi.org/10.1175/JAS-D-17-0150.1, https://doi.org/10.1175/JAS-D-17-0150.1.

Yang, D., 2019: Convective heating leads to self-aggregation by generating available potential energy. *Geophysical Research Letters*, **46 (0)**, doi:10.1029/2019GL083805, URL https://agupubs.onlinelibrary.wiley.com/doi/abs/10.1029/2019GL083805, https://agupubs.onlinelibrary.wiley.com/doi/pdf/10.1029/2019GL083805.

Yang, D., and A. P. Ingersoll, 2013: Triggered Convection, Gravity Waves, and the MJO: A Shallow-Water Model. *Journal of the Atmospheric Sciences*, **70 (8)**, 2476–2486, doi:10.1175/JAS-D-12-0255.1, URL http://dx.doi.org/10.1175/JAS-D-12-0255.1.

Yang, D., and A. P. Ingersoll, 2014: A theory of the MJO horizontal scale. *Geophysical Research Letters*, 661–666, doi:10.1002/2013GL058542, URL http://onlinelibrary.wiley.com/doi/10.1002/2013GL058542/epdf.

Yang, D., and S. D. Seidel, 2020: The incredible lightness of water vapor. *Journal of Climate*, **0 (0)**, null, doi:10.1175/JCLI-D-19-0260.1, URL https://doi.org/10.1175/JCLI-D-19-0260.1.

LIST OF FIGURES

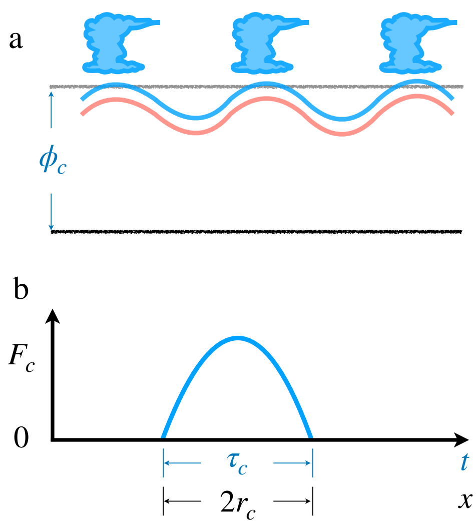

FIG. 1. Convection parameterization in the shallow water model. (a) Anomalously high geopotential triggers convection (the blue line); anomalously low geopotential does not trigger convection (the red line). (b) Convection acts as a mass sink in our model. Each convective storm occupies length of $2r_c$ and lasts for a time period of τ_c.

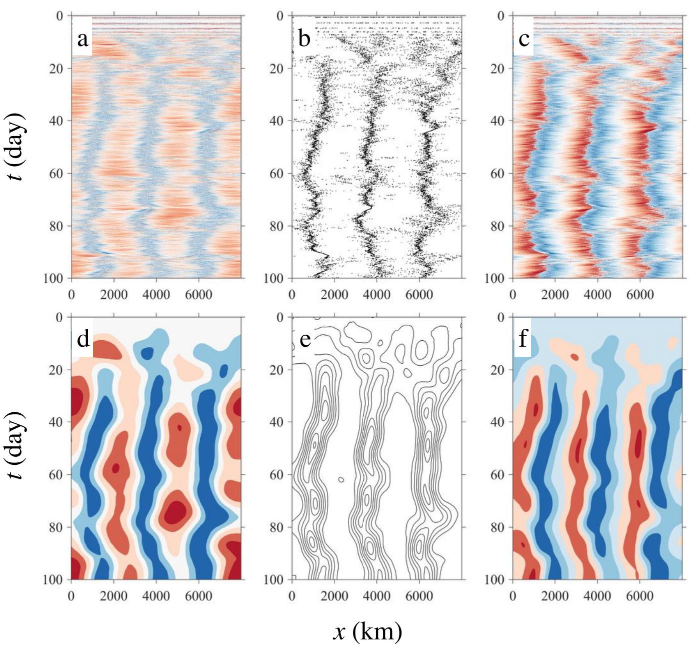

FIG. 2. The reference simulation. (a) Geopotential anomaly from its horizontal average ϕ' (m^2/s^2). (b) Convective heating F_c (m^2/s^3). (c) Horizontal wind u (m/s). (d-f) The slow components correspond to (a-c), respectively. The forcing amplitude is arbitrarily small. Therefore, the absolute value of our model output is not important.

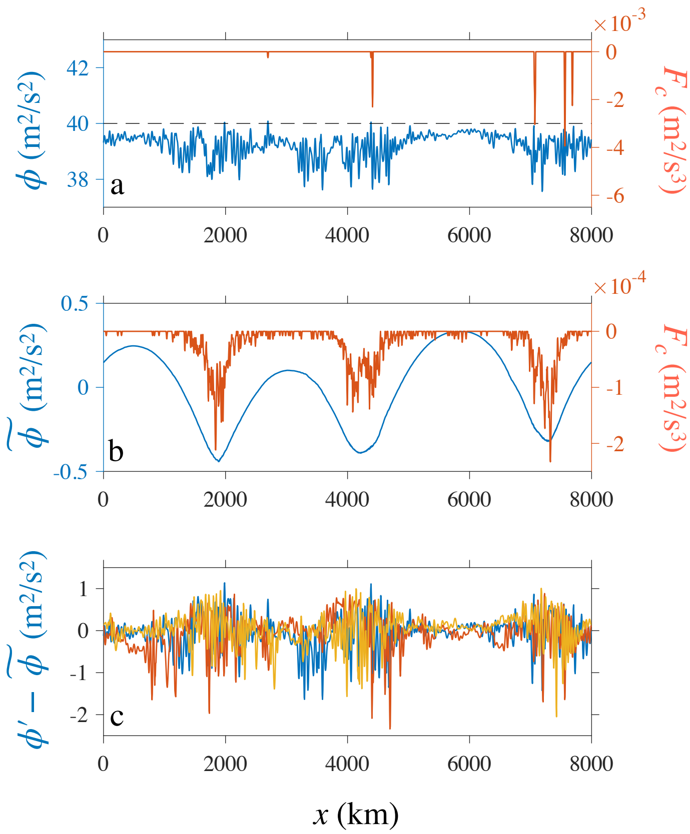

FIG. 3. The relation between ϕ and F_c at different scales. Locally, anomalously high ϕ triggers individual convective storms. However, these convective storms reside in a large-scale low pressure environment. (a) A snapshot of geopotential ϕ and convective heating F_c. (b) Slow components of ϕ and F_c. They are calculated as five-day averages. (c) Fast components of ϕ. Three snapshots with a one-day interval. Blue shows the time shown in (a), red shows one day earlier, and yellow shows one day later.

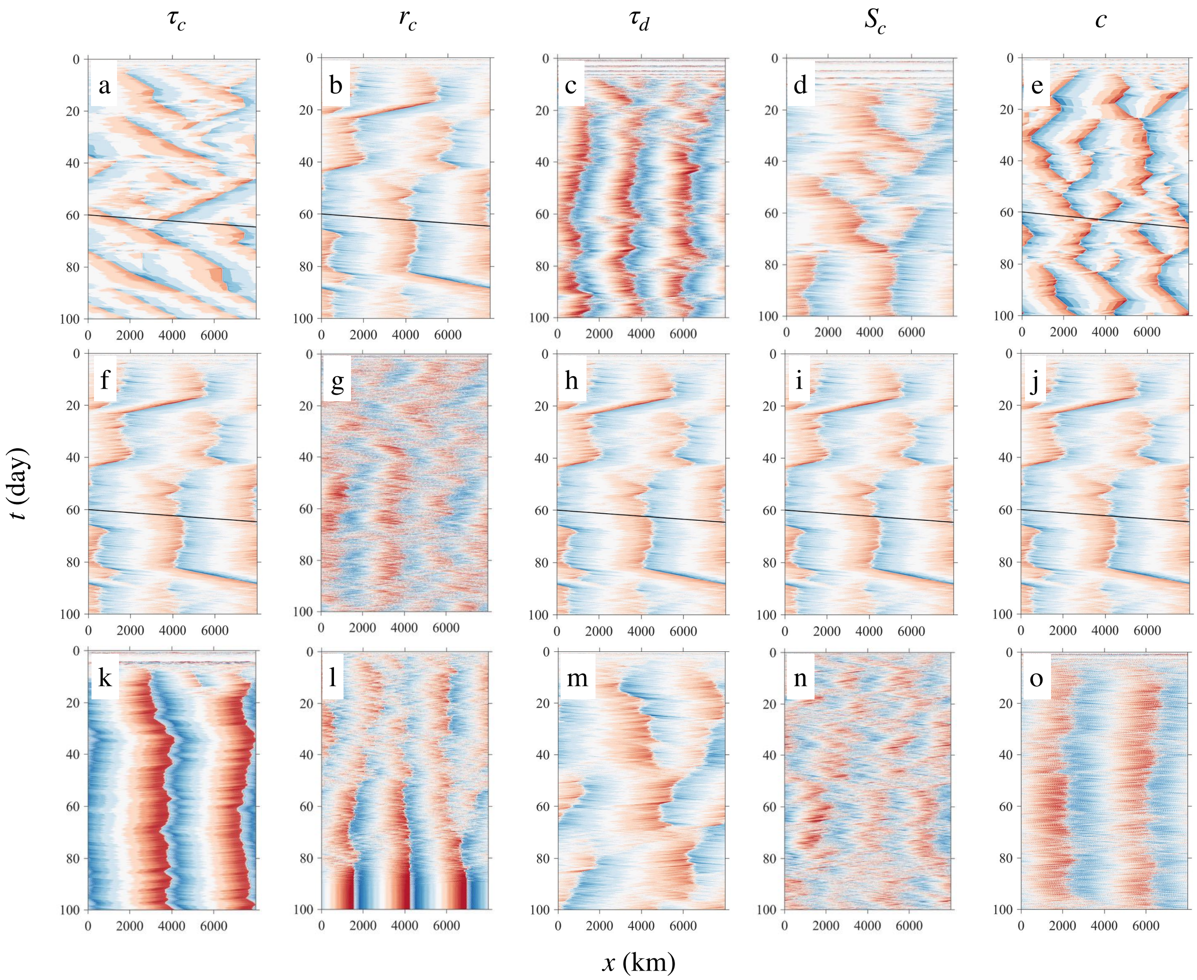

FIG. 4. Convective self-aggregation is simulated with a wide range of parameter values. Horizontal velocity u is shown in all panels. The first column presents simulations with $\tau_c = 0.4$, 0.6, and 1 hour, respectively. The second column presents simulations with $r_c = 10$, 20, and 40 km, respectively. The third column presents simulations with $\tau_d = 0.5$, 1, and 2 days, respectively. The fourth column presents simulations with $S_c = 2 \times 10^{-10},\ 4 \times 10^{-10},\ 8 \times 10^{-10}\ \mathrm{m^{-1}\ s^{-1}}$. The fifth column presents simulations with $c = 15,\ 20,\ 30$ m/s. We have varied each parameter at least by a factor of 2. All of the other parameters remain the same as in the reference simulation. The black lines provide the gravity wave speed in the corresponding simulations.

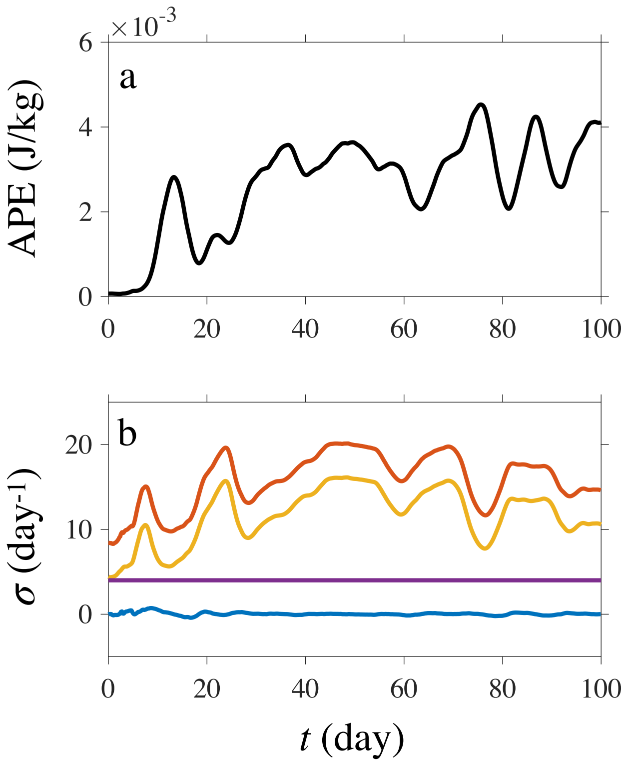

516 FIG. 5. (a) Temporal evolution of the available potential energy (APE). This is a model of linear dynamics, so the absolute magnitude of APE is not of importance. Instead, its increasing trend during the developing phase of self-aggregation is of interest. (b) The APE budget. Blue represents ∂_tAPE; red represents APE production due to convective heating; yellow represents APE conversion to KE; magenta represents sink of APE.